

# Theoretical Study on the Reaction of OH Radicals with Polychlorinated Dibenzo-*p*-dioxins

Jung Eun Lee and Wonyong Choi\*

*School of Environmental Science and Engineering/Department of Chemistry, Pohang University of Science and Technology, Pohang 790-784, Korea*

Byung Jin Mhin\*

*Department of Chemistry, PaiChai University, 493-6 Doma-dong, Seoku, Daejeon 302-735, Korea*

Krishnan Balasubramanian

*Department of Applied Science, University of California, Davis, Livermore, California 94550, USA, and Chemistry and Material Science Directorate, Lawrence Livermore National Laboratory, University of California, Livermore, California 94550, USA*

*Received: July 17, 2003; In Final Form: November 21, 2003*

Polychlorinated dibenzo-*p*-dioxins (PCDDs) are very harmful and toxic environmental pollutants. PCDDs emitted from various sources are chemically transformed and decomposed through reactions with the OH radicals in the atmosphere. The reaction mechanism for PCDD decomposition has not been understood completely because they are difficult to deal with due to their toxicities and very low vapor pressure. Therefore, we have carried out density functional theory calculations using the B3LYP/6-31G\*\* method for the initial OH radical reactions with four  $D_{2h}$  symmetric congeners, namely, dibenzo-*p*-dioxin (DD), 1,4,6,9-tetrachlorodibenzo-*p*-dioxin (1469-TCDD), 2,3,7,8-tetrachlorodibenzo-*p*-dioxin (2378-TCDD), and octachlorodibenzo-*p*-dioxin (OCDD) as reference compounds among 75 PCDDs to locate favorable reaction sites and reaction pathways for the first time. We found that the OH-substituted product (i.e., hydroxylated PCDD) is thermodynamically more stable than the PCDD–OH adduct. But the transition states for substitutions are higher than additions. The relative energies of the adducts and their transition states for the OH radical addition have negative values in terms of  $\Delta E_0$  in agreement with experimentally measured activation energy of DD. The OH radical addition to  $D_{2h}$  congeners can attack three different carbon sites, viz., oxygen-bonded carbon ( $C_7$ ),  $\alpha$ -position carbon ( $C_\alpha$ ), and  $\beta$ -position carbon ( $C_\beta$ ). Among three adduct isomers, the  $\gamma$  adduct, formed by the OH radical addition at an ether linkage carbon, is energetically more stable than the  $\alpha$  or  $\beta$  adducts. The first step for the OH radical addition into dioxin shows no significant dependence with the chlorination pattern. There is not much difference between 1469-TCDD and 2378-TCDD for the OH addition reaction. The geometrical parameters of the OH adduct show a marked change around the head carbon. But the structural parameters of the other unattacked benzene ring are nearly conserved after the OH radical addition.

## Introduction

Dioxin compounds are notorious for their biochemical and toxic effects.<sup>1,2</sup> Polychlorinated dibenzo-*p*-dioxins (PCDDs) produced from various sources are emitted and dispersed into the global environment.<sup>3–6</sup> In particular, a large quantity of PCDDs is emitted from the combustion of wastes in municipal incinerators.<sup>3–6</sup> PCDDs are persistent organic pollutants and transported or transformed through the atmosphere.<sup>7,8</sup> Physical, chemical, and biological properties of PCDDs show strong dependence on the position and the number of chlorines.<sup>9–14</sup> The PCDD homologue distribution is related with thermodynamic properties of PCDDs.<sup>14</sup>

PCDDs emitted into the atmosphere are transported in both particle-bound and gas phases.<sup>15,16</sup> Particle-phase PCDDs are removed from the atmosphere through the dry or wet deposition. The tropospheric removal or transformation of gas-phase PCDDs undergoes wet and dry deposition, photolysis, and reaction with

OH, HO<sub>2</sub>, and NO<sub>3</sub> radicals and O<sub>3</sub>. The wet and dry deposition of gaseous PCDDs seems to be of relatively minor importance as a removal pathway.<sup>15,16</sup> The reactions of PCDDs with the HO<sub>2</sub> radicals and O<sub>3</sub> in the troposphere are negligible as a removal pathway.<sup>15,16</sup> The reaction of NO<sub>3</sub> radicals with PCDDs is very slow.<sup>15,16</sup> The OH radical reactions with PCDDs are considered to be a dominant removal process in the atmosphere.<sup>17–19</sup>

The reaction of aromatic compounds with OH radicals undergoes one of these reactions as an initial step: (i) an H-atom abstraction from the substituent alkyl group of aromatic compounds; (ii) an addition of the OH radical to the benzene ring to form a hydroxycyclohexadienyl radical; (iii) an H-atom abstraction from the benzene ring; or (iv) a substitution of the substituent of the benzene ring.<sup>20,21</sup> In the high-temperature region (>600 K), the OH radicals react with aromatic compounds initially through H abstraction rather than OH addition into the benzene ring.<sup>20,21</sup> Under moderate atmospheric conditions, PCDDs initially react with the OH radicals to form PCDD–OH adduct radicals.<sup>15,19</sup> Toluene also undergoes an

\* Authors to whom correspondence should be addressed. E-mail: wchoi@postech.ac.kr (W.C.); mhin@mail.pcu.ac.kr (B.J.M.).

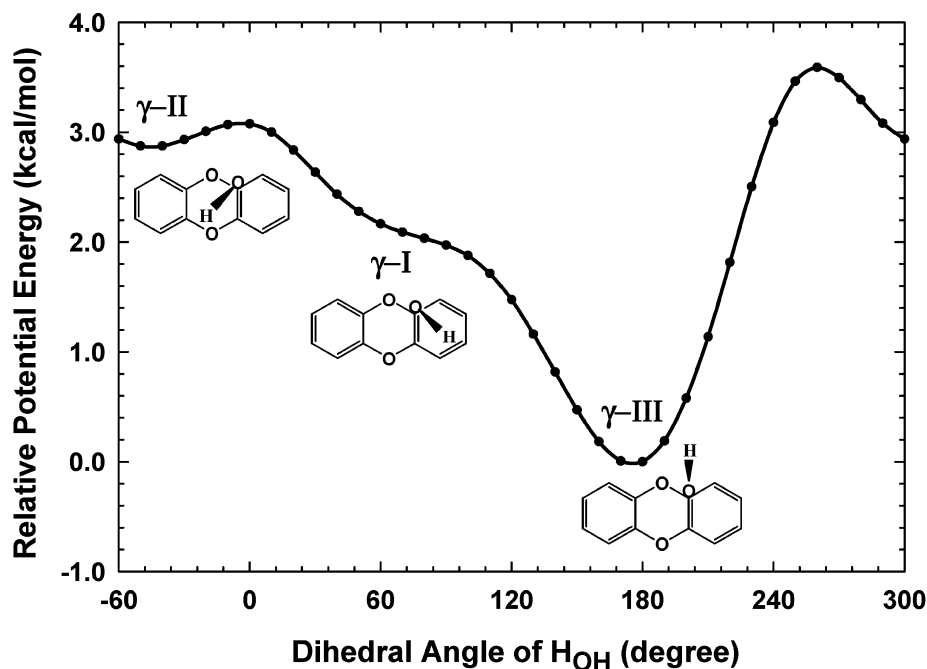


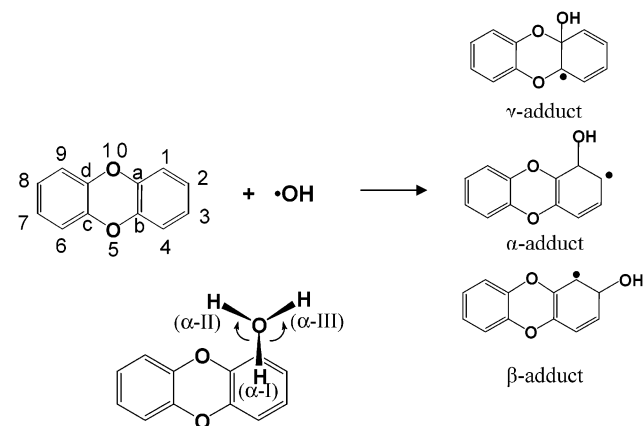
**Figure 1.** The relative potential energy (kcal/mol) of the  $\gamma$  conformer of the DD–OH adduct as a function of the rotating dihedral angle [ $\tau(\text{C}_b\text{C}_a\text{--OH}_{\text{OH}})$ ]. The three local minima ( $\gamma$ -I,  $\gamma$ -II, and  $\gamma$ -III) are equally separated by about  $120^\circ$ .

addition reaction with OH radicals by more than 90% in the atmosphere.<sup>22</sup> However, it is difficult to detect their intermediate radicals, that is, PCDD–OH adducts, and to deal with them due to their toxicity and the very low vapor pressure,  $10^{-4}$ – $10^{-11}$  Torr at 298 K.<sup>17–19</sup> The rate constant of degradation of PCDDs by OH radicals decreases with increase in the number of chlorine atoms.<sup>13,19</sup> The mechanism for the decomposition or transformation of gas-phase PCDDs is not understood well.<sup>23–25</sup> Previously the structure–reactivity methods<sup>20,21</sup> based on the electrophilic constants ( $\sigma_{\text{ortho}}$  or  $\sigma_{\text{para}}$ ,  $\sigma_{\text{meta}}$ ) were reported to estimate the OH radical rate constants of organic compounds with low vapor pressure such as PCDDs. In this work, we carried out density functional theory (DFT) calculations on the reaction of dibenzo-*p*-dioxin (DD), 1,4,6,9-tetrachlorodibenzo-*p*-dioxin (1469-TCDD), 2,3,7,8-tetrachlorodibenzo-*p*-dioxin (2378-TCDD), and octachlorodibenzo-*p*-dioxin (OCDD) with an OH radical to find out favorable reaction pathways and reaction sites in the gas phase.

### Computational Methods

We have performed DFT calculations using a Gaussian 98 suit of programs<sup>26</sup> at the level of DFT (B3LYP) with the 6-31G\*\* basis set for the PCDD–OH adducts, their transition states, and reactants. We have selected four  $D_{2h}$  symmetric congeners, DD, 1469-TCDD, 2378-TCDD, and OCDD, as reference compounds among all PCDD congeners. Physical and chemical properties of PCDDs are very sensitive to the number and position of chlorines.<sup>9–14</sup> Charge distributions of PCDDs (i.e., polarizabilities, quadrupole moments, and dipole moments) change very sensitively and systematically with the chlorination patterns.<sup>11</sup> The ring vibrational frequencies of PCDDs also change systematically with the chlorination pattern.<sup>12</sup> The vertical electron affinities<sup>27</sup> of PCDDs increase with an increasing number of chlorines. The reactivities of PCDD congeners are also very sensitive to the chlorination pattern. Therefore, we have selected the four  $D_{2h}$  symmetric congeners as representative molecules for the chlorination pattern to understand their reactivity toward the OH radicals.

### SCHEME 1. Addition of an OH Radical into Dibenzo-*p*-dioxin (DD) and the Formation of $\alpha$ , $\beta$ , and $\gamma$ Isomer Adducts and the Definition of Conformers I, II, and III for the $\alpha$ Adduct



A dioxin molecule is composed of 12 carbons, but these highly symmetric congeners have only three kinds of carbon sites. The OH radical addition to  $D_{2h}$  congeners can attack at three different carbon sites: oxygen-bonded carbon,  $\text{C}_a$ ,  $\text{C}_b$ ,  $\text{C}_c$ ,  $\text{C}_d$  ( $\text{C}_\gamma$ );  $\alpha$ -position carbon,  $\text{C}_1$ ,  $\text{C}_4$ ,  $\text{C}_6$ ,  $\text{C}_9$  ( $\text{C}_\alpha$ ); or  $\beta$ -position carbon,  $\text{C}_2$ ,  $\text{C}_3$ ,  $\text{C}_7$ ,  $\text{C}_8$  ( $\text{C}_\beta$ ) as shown in Scheme 1. Therefore, three kinds of adduct isomers,  $\gamma$ ,  $\alpha$ , and  $\beta$  adducts, are possible for the  $D_{2h}$  congeners. A PCDD–OH adduct may take many conformations through the rotation of the dihedral angle of hydroxyl-group hydrogen ( $\text{H}_{\text{OH}}$ ). We performed single-point energy calculations for the PCDD–OH adducts by rotating the dihedral angle of  $\text{H}_{\text{OH}}$  ( $\tau(\text{C}_b\text{C}_a\text{OH}_{\text{OH}})$ ) at an interval of  $10^\circ$  to find out the local minima on the potential-energy surface of the adduct conformer. Figure 1 shows three minimal points for the  $\gamma$  adduct of DD–OH at the dihedral angles ( $\tau$ ) of  $-60$ ,  $60$ , and  $180^\circ$ , which are equally separated by about  $120^\circ$ . On the basis of this figure, among a large number of OH-adduct conformers, the three conformers corresponding to the local minima were selected as the representatives; the conformation with  $\text{H}_{\text{OH}}$  oriented to the center of the benzene ring was

**TABLE 1: B3LYP/6-31G\*\***-Calculated  $E_e$  (Hartree),  $\Delta E_e$  (kcal/mol),  $\Delta E_0$  (kcal/mol),  $\Delta E_T$  (kcal/mol),  $\Delta H$  (kcal/mol),  $S$  (cal/mol K),  $\Delta S$  (cal/mol K),  $\Delta G$  (kcal/mol),  $\Delta H_f$  (kcal/mol) (at 298.15 K and 1 atm) of PCDD–OH Adducts and Transition States

PCDD + OH Adduct									
	$E_e$	$\Delta E_e$	$\Delta E_0$	$\Delta E_T$	$\Delta H$	$S$	$\Delta S$	$\Delta G$	$\Delta H_f$
DD									
$\alpha$ -I	−688.30017	−19.8	−16.5	−17.6	−18.2	108.1	−28.9	−9.6	−22.9
$\alpha$ -II	−688.29857	−18.8	−15.7	−16.6	−17.2	106.6	−30.4	−8.1	−21.9
$\alpha$ -III	−688.29553	−16.9	−14.0	−14.9	−15.4	109.7	−27.3	−7.3	−20.2
$\beta$ -I	−688.30282	−21.4	−18.1	−19.2	−19.8	108.0	−28.9	−11.2	−24.5
$\beta$ -II	−688.29818	−18.5	−15.5	−16.4	−17.0	108.1	−28.9	−8.4	−21.7
$\beta$ -III	−688.29793	−18.4	−15.4	−16.3	−16.9	108.1	−28.9	−8.3	−21.6
$\gamma$ -I	−688.30917	−25.4	−22.1	−23.3	−23.9	104.9	−32.1	−14.3	−28.6
$\gamma$ -II	−688.30836	−24.9	−21.7	−22.8	−23.4	105.2	−31.8	−14.0	−28.2
$\gamma$ -III	−688.31041	−26.2	−22.9	−24.1	−24.7	104.9	−32.0	−15.2	−29.5
1469-TCDD									
$\beta$ -I	−2526.66023	−22.0	−18.6	−19.6	−20.2	136.7	−29.0	−11.6	−40.2
$\beta$ -II	−2526.65833	−20.8	−17.6	−18.5	−19.1	136.8	−28.9	−10.5	−39.1
$\gamma$ -I	−2526.66896	−27.5	−24.1	−25.3	−25.9	133.3	−32.4	−16.2	−45.9
$\gamma$ -II	−2526.66749	−26.6	−23.4	−24.5	−25.0	133.8	−31.9	−15.5	−45.0
$\gamma$ -III	−2526.67266	−29.8	−26.3	−27.7	−28.3	133.3	−32.4	−18.6	−48.3
2378-TCDD									
$\alpha$ -I	−2526.66280	−21.1	−17.6	−18.7	−19.3	136.2	−29.0	−10.7	−42.0
$\alpha$ -II	−2526.66087	−19.9	−16.6	−17.5	−18.1	135.9	−29.4	−9.4	−40.8
$\alpha$ -III	−2526.66148	−20.3	−17.0	−17.9	−18.5	136.1	−29.2	−9.8	−41.2
$\gamma$ -I	−2526.67170	−26.7	−23.3	−24.5	−25.0	133.3	−31.9	−15.5	−47.8
$\gamma$ -II	−2526.67013	−25.7	−22.5	−23.6	−24.2	133.9	−31.4	−14.8	−46.9
$\gamma$ -III	−2526.67315	−27.6	−24.2	−25.4	−26.0	133.4	−31.8	−16.5	−48.7
OCDD									
$\gamma$ -I	−4365.00685	−28.9	−25.3	−26.5	−27.1	160.0	−32.4	−17.5	−49.6
$\gamma$ -II	−4365.00500	−27.7	−24.4	−25.4	−26.0	160.4	−31.9	−16.5	−48.5
$\gamma$ -III	−4365.01074	−31.3	−27.6	−29.0	−29.5	159.9	−32.5	−19.9	−52.0
Transition States									
DD									
$\alpha$ adduct	−688.27402	−3.4	−1.8	−1.9	−2.5	109.0	−28.0	5.82	
$\beta$ adduct	−688.27523	−4.1	−2.5	−2.7	−3.3	109.1	−27.9	5.06	
$\gamma$ adduct	−688.27627	−4.8	−2.2	−2.3	−2.9	108.9	−28.1	5.48	
1469-TCDD									
$\beta$ adduct	−2526.62931	−2.6	−1.2	−1.3	−1.8	137.8	−27.9	6.47	
$\gamma$ adduct	−2526.63053	−3.4	−1.9	−2.1	−2.7	135.7	−29.9	6.25	
2378-TCDD									
$\alpha$ adduct	−2526.63307	−2.4	−0.9	−1.0	−1.6	136.9	−28.4	6.82	
$\gamma$ adduct	−2526.63590	−4.2	−2.7	−2.9	−3.5	135.3	−29.9	5.40	
OCDD									
$\gamma$ adduct	−4364.96653	−3.6	−2.1	−2.3	−2.9	162.9	−29.4	5.92	

**TABLE 2: B3LYP/6-31G\*\***-Calculated  $E_e$  (Hartree),  $\Delta E_e$  (kcal/mol),  $\Delta E_0$  (kcal/mol),  $\Delta H$  (kcal/mol),  $S$  (cal/mol K),  $\Delta S$  (cal/mol K),  $\Delta G$  (kcal/mol),  $\Delta H_f$  (kcal/mol) (at 298.15 K and 1 Atm) of Substitution in PCDDs

	$E_e$	$\Delta E_e$	$\Delta E_0$	$\Delta H$	$S$	$\Delta S$	$\Delta G$	$\Delta H_f$
1469-TCDD								
$\alpha$ substitution	−2526.68702	−38.9	−34.9	−35.0	136.3	−29.3	−26.3	−55.0
TS	−2526.62341	1.1	2.4	2.3	136.9	−28.7	10.2	
2378-TCDD								
$\beta$ substitution	−2526.68936	−37.8	−34.0	−34.1	138.2	−27.0	−26.0	−56.8
TS	−2526.62748	1.1	2.4	2.3	136.4	−28.8	10.2	
OCDD								
$\alpha$ substitution	−4365.02320	−39.1	−35.2	−35.3	163.0	−29.3	−26.6	−57.8
$\beta$ substitution	−4365.01916	−36.6						

optimized, and then those with  $H_{OH}$  rotated by  $\pm 120^\circ$  were optimized. We define the geometry with  $H_{OH}$  oriented toward the benzene ring center as conformer I and the geometry with  $H_{OH}$  rotated by  $+120^\circ$  (clockwise) and by  $-120^\circ$  (counterclockwise) as conformers II and III, respectively. The barrier height for the OH internal rotation is calculated as the difference between the highest and lowest points on the potential curve in Figure 1. The energy barrier of the OH internal rotation for the  $\gamma$  adduct of DD (Figure 1) is estimated to be 3.6 kcal/mol. Throughout this work, all the calculations were performed for

these three representative conformers. For the OH adducts of DD, 2378-TCDD, and OCDD, we have reported the potential minima for each conformer I, II, and III. However, the optimized geometry of the  $\beta$ -III conformer for 1469-TCDD could not be obtained (hence, the data for the  $\beta$ -III conformer of 1469-TCDD are missing in Table 1) because geometry optimization of the  $\beta$ -III conformer resulted in a conversion to  $\beta$ -I through the rotation of  $H_{OH}$ .

The thermodynamic quantities, zero-point energies, and vibrational frequencies have been obtained from the optimized

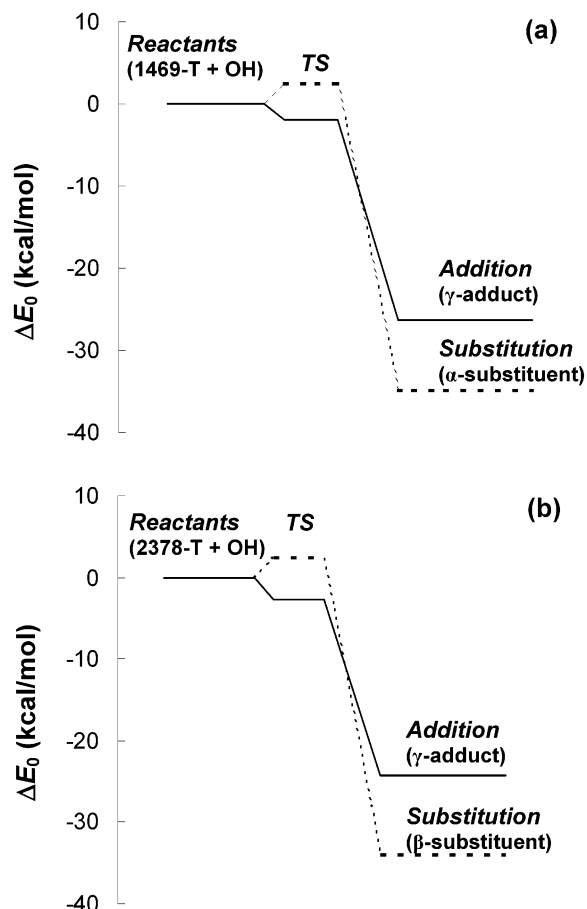


**Figure 2.** Comparison of addition and substitution reaction pathways for (a) 1469-TCDD and (b) 2378-TCDD with OH radical in terms of  $\Delta E_0$

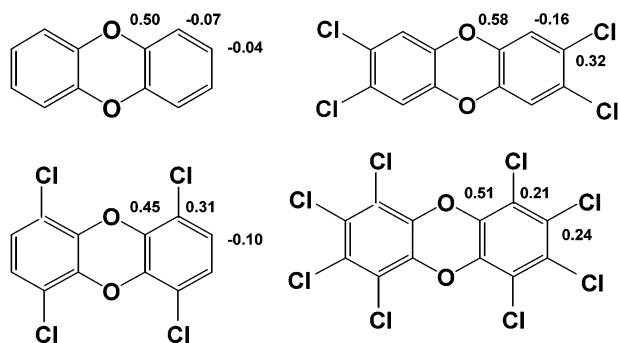
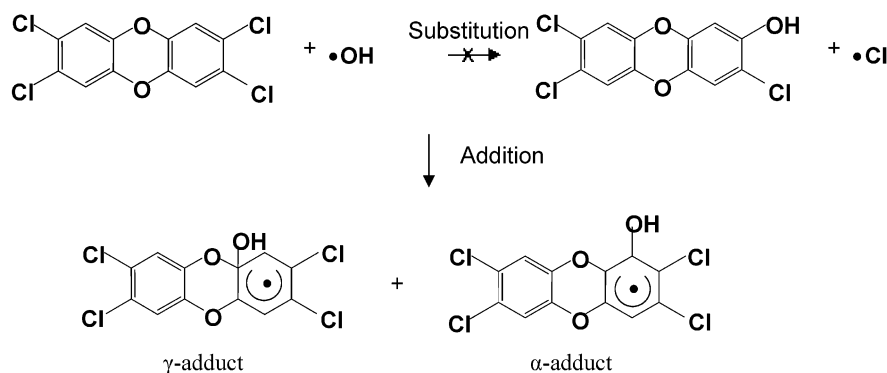


**Figure 3.** Carbon charge distributions calculated from the generalized atomic polar tensor (at  $\alpha$ ,  $\beta$ , and  $\gamma$  positions) of DD, 2378-TCDD, 1469-TCDD, and OCDD

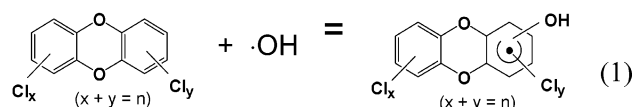
#### SCHEME 2. Addition vs Substitution for the Reaction of 2378-TCDD + OH



geometries under the rigid rotor and the harmonic oscillator approximation. The electronic energy ( $E_e$ ) and thermal energy ( $E_T = E_{zpe} + E_{vib} + E_{rot} + E_{trans}$ ) were calculated to get  $H$  ( $= E_e + E_T + RT$ ) at 298 K and 1 atm for the OH adduct. We have also calculated the transition states between the reactants and products to evaluate the activation energies. The optimized transition-state structure has one imaginary frequency corresponding to the C—O stretching vibration mode.

#### Thermodynamics for PCDD—OH Adduct Formation vs OH Substitution

We have carried out DFT calculations to get thermodynamic quantities for PCDD—OH adducts. The relative energies of the adducts and transition states with respect to reactants are listed in Table 1. We have also calculated the reaction enthalpies,  $\Delta H$ , and the formation enthalpies,  $\Delta H_f$ , for PCDD—OH adducts using the  $\Delta H_f$  values of PCDDs ( $\Delta H_f(\text{DD}) = -14.1$  kcal/mol,  $\Delta H_f(1469\text{-T}) = -29.4$  kcal/mol,  $\Delta H_f(2378\text{-T}) = -32.1$  kcal/mol,  $\Delta H_f(\text{OCDD}) = -31.9$  kcal/mol)<sup>14</sup> and OH radical ( $\Delta H_f(\text{OH}) = 9.4$  kcal/mol)<sup>28</sup> from eqs 2 and 3. Thermodynamic functions of  $\Delta E_e$  ( $= E_e(\text{product}) - E_e(\text{reactants})$ ) and  $\Delta E_0$  ( $= E_0(\text{product}) - E_0(\text{reactants})$ ,  $E_0 = E_e + E_{zpe}$ ), listed in Table 1, are calculated.  $\Delta S$  and  $\Delta G$  for the adducts are calculated from eqs 4 and 5, respectively.



$$\Delta H = H(\text{adduct}) - [H(\text{PCDD}) + H(\text{OH})] \quad (2)$$

$$\Delta H = \Delta H_f(\text{adduct}) - [\Delta H_f(\text{PCDD}) + \Delta H_f(\text{OH})] \quad (3)$$

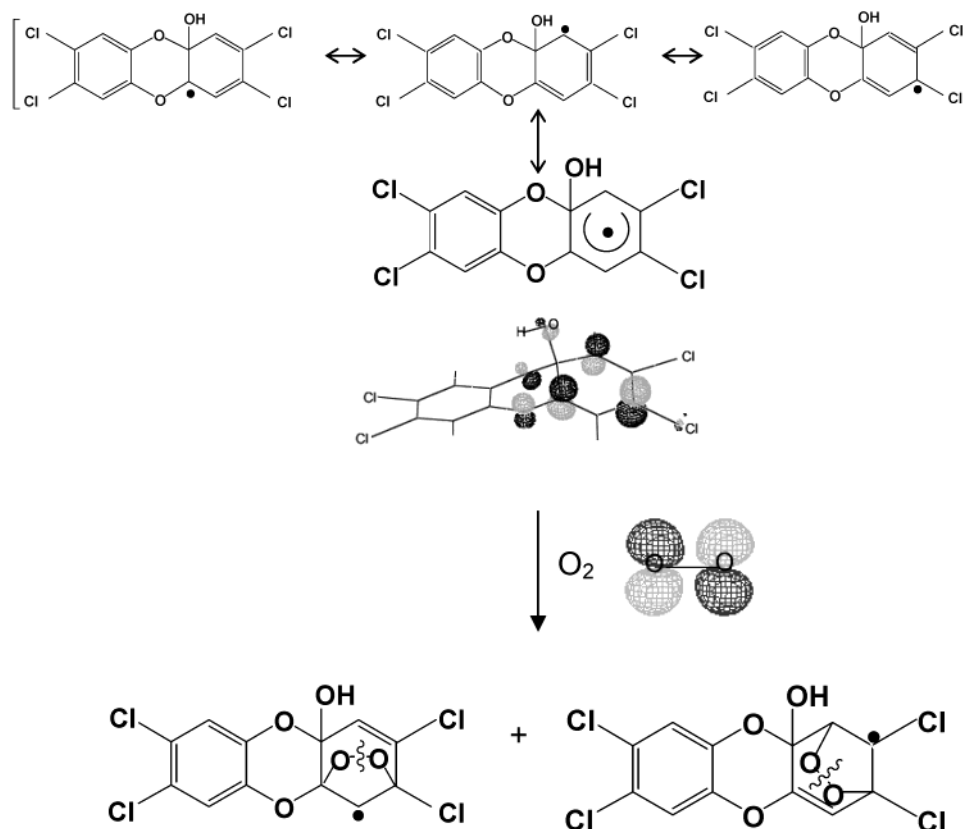
$$\Delta S = S(\text{adduct}) - S(\text{PCDD}) - S(\text{OH}) \quad (4)$$

$$[S(\text{adduct}) = S_{\text{elec}} + S_{\text{trans}} + S_{\text{vib}} + S_{\text{rot}} + S_{\text{torsion}}]$$

$$[S(\text{PCDD}) = S_{\text{elec}} + S_{\text{trans}} + S_{\text{vib}} + S_{\text{rot}}]$$

$$\Delta G = \Delta H(\text{adduct}) - T\Delta S \quad (5)$$

It may appear that the thermodynamic functions estimated in this work may have significant errors due to the classical approximation (the rigid rotor and harmonic oscillator treatment). In the low vibrational frequency region, the out-of-plane vibrational mode such as ring puckering should be considered as rotational motion and corrected in order to evaluate the entropy values.<sup>29–32</sup> The errors resulting from the out-of-plane, ring-puckering, ring-twisting, and butterfly vibrations in the low-frequency region ( $\leq 260$   $\text{cm}^{-1}$ ) significantly affect entropy and

**SCHEME 3.** A Probable Reaction Mechanism for O<sub>2</sub> Addition into the 2378-TCDD + OH Adduct and Molecular Orbitals of the Adduct (SOMO) and O<sub>2</sub> (HOMO)

the Gibbs free energy.<sup>29</sup> However, when using the isodesmic reaction 1 and eq 4, most entropy errors cancel out except for the OH internal rotation term that is absent in PCDD. Therefore, the internal rotation of the OH group in PCDD-OH adducts is treated as a torsional mode as in the case of benzene-OH adducts.<sup>33</sup> As a result, the  $S_{\text{vib}}$  term in  $S(\text{adduct})$  is the sum of 65 ( $= 3N - 7$ ) vibrational entropies and  $S_{\text{torsion}}$  is the entropy of the OH internal rotation. The reduced moment of inertia ( $I_{\text{OH}}$ ) for the OH rotational top is  $0.945 \pm 0.005 \text{ amu } \text{\AA}^2$  for all PCDD-OH adducts.  $S_{\text{torsion}}$  for PCDD-OH adducts is about 2.4 cal/mol K. The entropy difference between PCDD and the PCDD-OH adducts for the ring puckering ( $B_{3u}$ ) in the low-frequency region is less than 0.5 cal/mol K, which induces an error of less than 0.15 kcal/mol in Gibbs free energy. Hence, although nonrigid treatment appears to be important for the absolute free energies and entropies, relative free energies of the reactions are not affected by this as the entropy errors due to nonrigidity cancel out.

All PCDD-OH adducts are energetically more stable than the reactants PCDD + OH. The relative energy of the adduct with respect to reactants has a negative value. DD can have three kinds of isomers,  $\gamma$ -,  $\alpha$ -, and  $\beta$ -adduct isomers. The  $\gamma$  adducts are energetically more stable than  $\alpha$  or  $\beta$  adducts. Among  $\alpha$  and  $\beta$  isomers, conformer I is more stable than II and III. For the  $\gamma$  adducts, conformer III is more stable than I and II. The  $\gamma$ -III conformer is more stable than  $\alpha$ -I and  $\beta$ -I by 6.4 and 4.8 kcal/mol, respectively, in terms of  $\Delta E_0$ . The most stable conformers are  $\alpha$ -I,  $\beta$ -I, and  $\gamma$ -III, which have the geometries with the dihedral angle of  $\text{H}_{\text{OH}}$  [ $\tau(\text{H}_1\text{C}_1\text{OH}_{\text{OH}})$  for the  $\alpha$  adduct,  $\tau(\text{H}_2\text{C}_2\text{OH}_{\text{OH}})$  for the  $\beta$  adduct, and  $\tau(\text{C}_6\text{C}_a\text{OH}_{\text{OH}})$  for the  $\gamma$  adduct] nearly  $180^\circ$ .

The same tendency is observed for the OH adducts of 1469-TCDD, 2378-TCDD, and OCDD. The  $\gamma$  adducts are energeti-

cally more stable than the  $\alpha$  or  $\beta$  adducts. Conformer  $\gamma$ -III is more stable than the other conformers. For 1469-TCDD adducts, the  $\gamma$ -III conformer is more stable than  $\beta$ -I by 7.7 kcal/mol in terms of  $\Delta E_0$ . The  $\gamma$ -III adduct of 2378-TCDD is more stable than  $\alpha$ -I by 6.6 kcal/mol in terms of  $\Delta E_0$ . OCDD has only one kind of available carbon,  $\text{C}_\gamma$ , for the OH radical addition. More chlorinated dioxins can form more stable OH adducts. The  $\gamma$ -III conformer of OCDD is energetically the most stable of all in Table 1.

For these PCDD congeners, the attack of the OH radical at the chlorinated carbon site results in the substitution of a chlorine atom. The total energies and relative thermodynamic functions for the OH substituted dioxins and their transition states are listed in Table 2. The OH radical substituted dioxins are more stable than the addition products, but the transition states are higher with respect to the reactants as shown in Figure 2. The activation energies for the OH substitution at the  $\alpha$  position of 1469-TCDD and at the  $\beta$  position of 2378-TCDD are positive, whereas the activation energies for the OH addition at the  $\alpha$  position of 2378-TCDD and at the  $\beta$  position of 1469-TCDD are negative. Therefore, the addition of an OH radical into PCDD is more favorable than substitution.

### Geometrical Parameters

All carbons in PCDDs have double-bond character. After the OH radical addition, the head carbon has near single bond character, which is distinguishable from the reactant. Table 3 shows that the geometry around the head carbon to which the OH radical is added changes obviously. But the structure of the other unattacked benzene ring is conserved. The OH radical addition affects only the attacked benzene ring.

The geometrical parameters for the conformers  $\alpha$ -I,  $\beta$ -I, and  $\gamma$ -III of DD, 1469-TCDD, 2378-TCDD, and OCDD are listed



**TABLE 3: Calculated Geometrical Parameters at the Level of B3LYP/6-31G\*\* for Reactants and  $\alpha$ -I,  $\beta$ -I, and  $\gamma$ -III Conformers of DD, 1469-TCDD, 2378-TCDD, and OCDD**

	reactants					$\alpha$ -I adducts		$\beta$ -I adducts		$\gamma$ -III adducts			
	OH	DD	1469-T	2378-T	OCDD	DD	2378-T	DD	1469-T	DD	1469-T	2378-T	OCDD
$\alpha$ Adduct													
$r(\text{C}_1\text{O})^b$						1.446	1.434						
$\angle \text{C}_a\text{C}_1\text{O}$						111.4	111.2						
$\angle \text{C}_1\text{OH}$						106.3	107.4						
$\tau(\text{X}_1\text{C}_1\text{OH})$						174.5	175.6						
$\beta$ Adduct													
$r(\text{C}_2\text{O})$								1.449	1.436				
$\angle \text{C}_1\text{C}_2\text{O}$								111.2	112.2				
$\angle \text{C}_2\text{OH}$								106.1	107.2				
$\tau(\text{X}_2\text{C}_2\text{OH})$								-178.7	-179.5				
$\gamma$ Adduct													
$r(\text{C}_a\text{O})$										1.421	1.405	1.414	1.401
$\angle \text{O}_{10}\text{C}_a\text{O}$										108.3	109.0	108.6	109.1
$\angle \text{C}_a\text{OH}$										107.2	107.5	107.8	107.8
$\tau(\text{C}_b\text{C}_a\text{OH})$										177.8	-179.9	176.4	179.6
$r(\text{OH})$	0.980					0.969	0.969	0.969	0.969	0.970	0.971	0.970	0.971
Center Ring													
$r(\text{O}_{10}\text{C}_a)$		1.381	1.374	1.378	1.373	1.369	1.368	1.383	1.377	1.449	1.450	1.449	1.452
$r(\text{O}_{10}\text{C}_d)$		1.381	1.374	1.378	1.373	1.384	1.381	1.376	1.369	1.374	1.367	1.371	1.366
$r(\text{O}_5\text{C}_b)$		1.381	1.374	1.378	1.373	1.388	1.387	1.368	1.362	1.362	1.357	1.361	1.357
$r(\text{O}_5\text{C}_c)$		1.381	1.374	1.378	1.373	1.379	1.376	1.380	1.372	1.381	1.373	1.378	1.372
$\angle \text{C}_a\text{O}_{10}\text{C}_d$	116.4	117.2	116.1	117.2	116.3	116.0	117.5	118.1	113.3	113.2	113.2	113.1	113.2
$\angle \text{C}_b\text{O}_5\text{C}_c$	116.4	117.2	116.1	117.2	116.1	115.8	117.2	118.0	117.6	118.0	117.3	118.1	118.1
$\angle \text{O}_{10}\text{C}_a\text{C}_b$	121.8	121.4	121.9	121.4	122.7	122.9	120.0	119.9	109.7	108.0	109.7	107.8	107.8
$\angle \text{C}_a\text{C}_b\text{O}_5$	121.8	121.4	121.9	121.4	121.6	121.8	122.0	121.5	116.6	115.7	116.8	115.8	115.8
$\angle \text{C}_c\text{C}_d\text{O}_{10}$	121.8	121.4	121.9	121.4	121.3	121.5	122.0	121.6	120.9	120.4	121.0	120.3	120.3
$\angle \text{O}_5\text{C}_c\text{C}_d$	121.8	121.4	121.9	121.4	121.8	122.0	121.3	121.0	121.1	120.7	121.2	120.7	120.7
Attacked Benzene Ring													
$r(\text{C}_a\text{C}_b)$		1.400	1.400	1.399	1.394	1.378	1.375	1.429	1.425	1.503	1.507	1.501	1.500
$r(\text{C}_a\text{C}_1)$		1.390	1.395	1.387	1.395	1.501	1.501	1.357	1.365	1.496	1.504	1.495	1.504
$r(\text{C}_4\text{C}_b)$		1.390	1.395	1.387	1.395	1.399	1.398	1.410	1.418	1.370	1.370	1.365	1.368
$r(\text{C}_3\text{C}_4)$		1.397	1.396	1.398	1.406	1.424	1.422	1.366	1.362	1.408	1.410	1.412	1.423
$r(\text{C}_1\text{C}_2)$		1.397	1.396	1.398	1.406	1.503	1.513	1.502	1.507	1.363	1.365	1.362	1.370
$r(\text{C}_2\text{C}_3)$		1.400	1.390	1.400	1.404	1.363	1.369	1.505	1.506	1.422	1.414	1.431	1.433
$r(\text{C}_1\text{X}_1)^a$		1.085	1.744	1.083	1.733	1.100	1.098	1.085	1.734	1.086	1.745	1.084	1.734
$r(\text{C}_4\text{X}_4)^a$		1.085	1.744	1.083	1.733	1.083	1.082	1.086	1.751	1.085	1.748	1.083	1.738
$r(\text{C}_2\text{X}_2)^a$		1.085	1.083	1.745	1.735	1.085	1.734	1.101	1.099	1.086	1.084	1.750	1.739
$r(\text{C}_3\text{X}_3)^a$		1.085	1.083	1.745	1.735	1.086	1.750	1.085	1.083	1.084	1.083	1.733	1.723
$\angle \text{C}_b\text{C}_a\text{C}_1$	120.1	119.9	120.1	120.4	123.1	123.2	121.2	121.0	112.4	111.9	112.3	112.3	112.3
$\angle \text{C}_4\text{C}_b\text{C}_a$	120.1	119.9	120.1	120.4	121.1	121.1	120.1	119.7	123.0	122.8	123.0	123.6	123.6
$\angle \text{C}_a\text{C}_1\text{C}_2$	119.9	120.1	120.2	119.7	111.8	111.5	122.4	122.7	121.5	122.6	121.9	122.2	122.2
$\angle \text{C}_3\text{C}_4\text{C}_b$	119.9	120.1	120.2	119.7	119.3	119.5	120.7	121.1	119.9	120.5	120.2	120.1	120.1
$\angle \text{C}_1\text{C}_2\text{C}_3$	120.0	120.1	119.8	119.9	122.5	122.1	112.9	112.3	121.5	121.1	121.1	120.9	120.9
$\angle \text{C}_2\text{C}_3\text{C}_4$	120.0	120.1	119.8	119.9	121.8	121.6	122.7	122.9	120.2	120.3	119.9	119.9	119.9
$\angle \text{C}_a\text{C}_1\text{X}_1^a$	118.4	119.6	119.3	118.5	108.5	109.0	119.5	120.6	116.1	115.4	116.9	114.4	114.4
$\angle \text{C}_b\text{C}_4\text{X}_4^a$	118.4	119.6	119.3	118.5	118.9	119.8	117.7	118.2	118.8	120.0	119.7	118.9	118.9
$\angle \text{C}_1\text{C}_2\text{X}_2^a$	119.6	119.3	118.5	119.7	116.0	114.9	109.7	108.7	119.5	119.5	118.9	119.9	119.9
$\angle \text{C}_4\text{C}_3\text{X}_3^a$	119.6	119.3	118.5	119.7	118.4	116.6	120.6	120.4	119.7	119.3	118.5	119.8	119.8
$\tau(\text{O}_5\text{C}_b\text{C}_a\text{C}_1)$	180.0	180.0	180.0	180.0	-177.0	-175.6	179.7	179.3	-169.3	-171.3	-168.7	-170.6	-170.6
$\tau(\text{O}_{10}\text{C}_a\text{C}_b\text{C}_4)$	180.0	0.0	180.0	180.0	-177.9	-177.8	179.3	178.6	132.5	128.1	132.6	128.2	128.2
$\tau(\text{C}_b\text{C}_a\text{C}_1\text{C}_2)$	0.0	0.0	0.0	0.0	-6.7	-10.6	2.1	-3.3	-12.7	-9.7	-14.0	-10.7	-10.7
$\tau(\text{C}_a\text{C}_b\text{C}_4\text{C}_3)$	0.0	0.0	0.0	0.0	0.4	1.3	0.7	0.2	-5.3	-4.0	-5.1	-3.6	-3.6
$\tau(\text{O}_{10}\text{C}_a\text{C}_1\text{X}_1)^a$	0.0	0.0	0.0	0.0	52.0	51.4	-0.1	-0.7	49.3	57.5	48.8	56.9	56.9
$\tau(\text{O}_5\text{C}_b\text{C}_4\text{X}_4)^a$	0.0	0.0	0.0	0.0	0.8	1.4	0.2	1.0	-1.0	-1.1	-0.9	-1.0	-1.0
$\tau(\text{C}_a\text{C}_1\text{C}_2\text{X}_2)^a$	180.0	180.0	180.0	180.0	-177.0	-172.6	-125.6	127.9	-175.8	-175.3	-175.0	-174.9	-174.9
$\tau(\text{C}_b\text{C}_4\text{C}_3\text{X}_3)^a$	180.0	0.0	180.0	180.0	179.1	177.5	-179.4	180.0	180.0	179.9	178.4	177.9	177.9

<sup>a</sup> X = H or Cl atom. <sup>b</sup> Bond length in Å.

in Table 3. The bond length of the OH group in the adducts,  $r_{\text{OH}}$ , decreases by 0.01 Å compared to the free hydroxyl radical. The bond lengths  $r_{\text{C}_a\text{OH}}$  are 1.40–1.42 Å for the  $\gamma$  adducts, which are shorter than those,  $r_{\text{C}_1\text{OH}}$  or  $r_{\text{C}_2\text{OH}}$ , 1.43–1.45 Å for the  $\alpha$  or  $\beta$  adducts. The bond distance  $r_{\text{CO}}$  increases slightly by increasing the chlorination level within the same adduct group. The structural difference of the  $\alpha$  or  $\beta$  adduct is seen near the head carbon ( $\text{C}_1$  or  $\text{C}_2$ ). The bond lengths linked to the head carbon,  $r_{\text{CC}}$  and  $r_{\text{CH}}$ , increase by 0.1 and 0.02 Å, respectively. The angles of  $\angle \text{CCC}$  and  $\angle \text{CCH}$  of the head carbon decrease by 8 and 10° for the  $\alpha$ - and  $\beta$ -OH adducts.

For the  $\gamma$  adducts, the bond lengths around the  $\text{C}_a$ ,  $r_{\text{C}_a\text{C}_b}$ ,  $r_{\text{C}_a\text{C}_1}$ , and  $r_{\text{C}_a\text{O}_{10}}$ , increase by 0.10, 0.10, and 0.07 Å, respectively. The angles of  $\angle \text{O}_{10}\text{C}_a\text{C}_1$  and  $\angle \text{C}_b\text{C}_a\text{C}_1$  decrease by about 12 and 8° for the  $\gamma$  adducts. The dihedral angles  $\tau(\text{O}_{10}\text{C}_a\text{C}_1\text{X}_1)$  are more than 49° and the planarity of the  $D_{2h}$  symmetric congeners breaks.

The geometrical parameters around the head carbon in the OH radical added benzene ring are quite different from PCDD, while the structural parameters for the other benzene ring show little difference. The OH radical addition into PCDD has little influence on the other unattacked benzene ring (Supporting

Information, Table 1S). At the transition state, the distance between PCDD and OH,  $r_{\text{CO}}$ , is 2.11–2.13 Å for the  $\gamma$  adducts while the distances are 2.06–2.08 Å for  $\alpha$ - and  $\beta$ -OH adducts.

### IR Vibrational Frequencies of PCDD–OH Adducts

The differences in structural parameters are consistent with the observed in their calculated IR spectra, which are listed in Supporting Information (Table 2S). PCDDs with  $D_{2h}$  symmetry, DD, 1469-TCDD, 2378-TCDD, and OCDD, have 60 vibrational modes:  $11A_g + 5A_u + 4B_{1g} + 5B_{2g} + 10B_{3g} + 10B_{1u} + 10B_{2u} + 5B_{3u}$ .<sup>34</sup> The PCDD–OH adducts have 6 additional modes associated with the C–OH group. The C–OH stretching of the adduct appears in the region of 980–1100  $\text{cm}^{-1}$  with strong intensity. This strong vibration band could be used for identifying the adducts. The O–H stretching vibration for these adducts appears at around 3750–3805  $\text{cm}^{-1}$ , which is blueshifted from 3694  $\text{cm}^{-1}$  of the free OH radical. The hydrogen bending vibrations of the C–O–H group for the  $\gamma$  adducts are observed with strong intensity in the region of 1000–1100  $\text{cm}^{-1}$  compared with the  $\alpha$  or  $\beta$  adducts. The C–H stretching vibration<sup>12</sup> of reactant PCDDs can be observed in the frequency region  $\geq 3200 \text{ cm}^{-1}$ , while the  $\text{C}_{\text{OH}}\text{--H}$  stretching vibration appears at 2900–3000  $\text{cm}^{-1}$  for the  $\alpha$  and  $\beta$  adducts because of the change of the head carbon into single-bond character. There is little difference in the C–H stretching vibration between the reactant and adduct for the  $\gamma$  adducts. In our previous study,<sup>12</sup> the IR spectrum for DD showed two ring-stretching vibrations ( $B_{2u}$ ) at 1538 and 1642  $\text{cm}^{-1}$  with strong intensity. These ring-stretching bands attributed to the unattacked benzene ring of the DD–OH adducts appear in the same region. However, the intensity of the spectrum reduces and the main peak is split into several peaks. Two benzene rings are not the same after the addition of the OH radical. For 1469-TCDD, 2378-TCDD, and OCDD, similar trends can be seen in their IR spectra. Calculated transition states have only one imaginary frequency corresponding to the C–O bonding formation for all transition states (Supporting Information, Table 3S).

### Conclusions

On the basis of the DFT calculation results on the reaction of PCDD with an OH radical, the substitution products are thermodynamically more stable than the adducts. But the transition states for the substitution are higher than those for the addition. Relative energies of transition states of OH radical addition have slightly negative values; there is no energy barrier to form PCDD–OH adducts. Brubaker and Hites<sup>19</sup> have carried out experiments to measure the OH radical rate constants for polycyclic aromatic hydrocarbons and dioxin congeners. According to their results, the activation energy barrier for the OH radical addition into DD has a slight negative value ( $-0.29 \pm 0.49 \text{ kJ/mol}$ ). Therefore, under moderate atmospheric conditions, the addition of an OH radical into a PCDD congener should be more favorable than the substitution as shown in Scheme 2.

In the present calculation results, there is no dependency on the chlorination pattern of PCDD for the first OH radical addition step, though the structure–reactivity methods<sup>15,16</sup> for the OH addition at the  $\alpha$ -, or  $\beta$ -position based on the electrophilic constants ( $\sigma_{\text{ortho}}$  and  $\sigma_{\text{meta}}$ ) showed a little difference according to the chlorination pattern. There is no great difference between 1469-TCDD and 2378-TCDD in comparing their  $\gamma$  adducts. Among three kinds of DD–OH adduct isomers, the  $\gamma$  isomers are more stable than  $\alpha$  or  $\beta$  isomers. Among all carbon sites in PCDDs, oxygen-bonded carbon  $C_\gamma$  has the most positive charge and should be reactive toward nucleophilic species.

Figure 3 shows the generalized atomic charge distributions obtained from atomic polar tensors for three kinds of carbons ( $\alpha$ -,  $\beta$ -, and  $\gamma$ ) in DD, 1469-TCDD, 2378-TCDD, and OCDD. For all congeners, the  $C_\gamma$  site has less electron density and is the most positive. The hydroxyl radical is known to be both nucleophilic and electrophilic in its reactions, and the oxygen in OH carries a partial negative charge to react with more positive carbon sites.<sup>35</sup> Therefore, the  $C_\gamma$  site might be regioselective for the initial OH addition.

Experimental results showed that the rate constants of PCDD + OH radicals decrease by increasing the number of chlorines. It seems that the first step, the OH radical addition into PCDD, does not play an important role in determining the overall decomposition rate.<sup>17–19,23–25</sup> The rate-determining step would be one of the next steps following the OH radical addition. In general, the OH radical adduct, a carbon-centered radical, should immediately react with  $\text{O}_2$  to complete the decomposition process. Scheme 3 shows the possible sites to react with  $\text{O}_2$  for the  $\gamma$  adduct of 2378-TCDD + OH. The ortho and para positions have the most favorable molecular orbitals for the addition of  $\text{O}_2$ . Further reactions should take place after the cleavage of the O–O bond. More studies on these reactions are needed to investigate the whole reaction pathways for the dioxin decomposition in the atmosphere.

**Acknowledgment.** We thank the financial support from the KOSEF (Grant No. R-14-2002-004-01001-0), the Center for Integrated Molecular Systems, and the Brain Korea 21 Project. The research at UC Davis was supported in part by the U.S. National Science Foundation Grant CHE-0236434.

**Supporting Information Available:** Tables of calculated geometrical parameters, the rotational constants, IR frequencies, and intensities for PCDD and PCDD–OH adducts in a PDF. This material is available free of charge via the Internet at <http://pubs.acs.org>.

### References and Notes

- (1) *Chlorinated Dioxins and Dibenzofurans in the Total Environment*; Choudhary, G., Keith, L. H., Rappe, C., Eds.; Butterworth Publishers: Boston, 1983.
- (2) *Dioxin and Health*; Schechter, A., Ed.; Plenum Press: New York, 1994.
- (3) Olie, K.; Vermeulen, P. L.; Hutzinger, O. *Chemosphere* **1977**, *6*, 455.
- (4) Bacher, R.; Swerev, M.; Ballschmiter, B. *Environ. Sci. Technol.* **1992**, *26*, 1649.
- (5) Addink, R.; Govers, H. A. J.; Olie, K. *Environ. Sci. Technol.* **1998**, *32*, 1888.
- (6) Yasuhara, A.; Katami, T.; Okuda, T.; Ohno, N.; Shibamoto, T. *Environ. Sci. Technol.* **2001**, *35*, 1373.
- (7) Lynam, M. M.; Kutty, M.; Damborsky, J.; Koca, J.; Adriaens, P. *Environ. Toxicol. Chem.* **1998**, *17*, 988.
- (8) Baker, J. I.; Hites, R. A. *Environ. Sci. Technol.* **2000**, *34*, 2879.
- (9) Safe, S. *Crit. Rev. Toxicol.* **1990**, *21*, 51.
- (10) Mason, G.; Farrell, K.; Keys, B.; Piskorska-Pliszczynska, J.; Safe, L.; Safe, S. *Toxicology* **1986**, *41*, 21.
- (11) Mhin, B. J.; Lee, J. E.; Choi, W. *J. Am. Chem. Soc.* **2002**, *124*, 144.
- (12) Mhin, B. J.; Choi, J.; Choi, W. *J. Am. Chem. Soc.* **2001**, *123*, 3584.
- (13) Choi, W.; Hong, S. J.; Chang, Y.-S.; Cho, Y. *Environ. Sci. Technol.* **2000**, *34*, 4810.
- (14) Lee, J. E.; Choi, W.; Mhin, B. J. *J. Phys. Chem. A* **2003**, *107*, 2693.
- (15) Atkinson, R. In *Issues in Environmental Science and Technology*; Hester, R. E., Harrison, R. M., Eds.; The Royal Society of Chemistry: Cambridge, UK, 1996; Vol. 6, p 53.
- (16) Kwok, E. S. C.; Atkinson, R. *Atmos. Environ.* **1995**, *29*, 1685.
- (17) Brubaker, W. W.; Hites, R. A. *Environ. Sci. Technol.* **1997**, *31*, 1805.
- (18) Kwok, E. S. C.; Arey, J.; Atkinson, R. *Environ. Sci. Technol.* **1994**, *28*, 528.

- (19) Brubaker, W. W.; Hites, R. A. *J. Phys. Chem. A* **1998**, *102*, 915.
- (20) Atkinson, R. *Atmos. Environ.* **1990**, *24A*, 1.
- (21) Atkinson, R. *Chem. Rev.* **1986**, *86*, 69.
- (22) Seinfeld, J. H. *Atmospheric Chemistry and Physics of Air Pollution*; John Wiley & Sons: New York, 1986.
- (23) Addink, R.; Olie, K. *Environ. Sci. Technol.* **1995**, *29*, 1425.
- (24) Ritter, E. R.; Bozzelli, J. W. *Combust. Sci. Technol.* **1994**, *101*, 153.
- (25) Guan, B.; Wan, P. *J. Photochem. Photobiol., A* **1994**, *80*, 199.
- (26) Frisch, M. J.; Trucks, G. W.; Schlegel, H. B.; Scuseria, G. E.; Robb, M. A.; Cheeseman, J. R.; Zakrzewski, V. G.; Montgomery, J. A., Jr.; Stratmann, R. E.; Burant, J. C.; Dapprich, S.; Millam, J. M.; Daniels, A. D.; Kudin, K. N.; Strain, M. C.; Farkas, O.; Tomasi, J.; Barone, V.; Cossi, M.; Cammi, R.; Mennucci, B.; Pomelli, C.; Adamo, C.; Clifford, S.; Ochterski, J.; Petersson, G. A.; Ayala, P. Y.; Cui, Q.; Morokuma, K.; Malick, D. K.; Rabuck, A. D.; Raghavachari, K.; Foresman, J. B.; Cioslowski, J.; Ortiz, J. V.; Stefanov, B. B.; Liu, G.; Liashenko, A.; Piskorz, P.; Komaromi, I.; Gomperts, R.; Martin, R. L.; Fox, D. J.; Keith, T.; Al-Laham, M. A.; Peng, C. Y.; Nanayakkara, A.; Gonzalez, C.; Challacombe, M.; Gill, P. M. W.; Johnson, B. G.; Chen, W.; Wong, M. W.; Andres, J. L.; Head-Gordon, M.; Replogle, E. S.; Pople, J. A. *Gaussian 98*, revision A.9; Gaussian, Inc.: Pittsburgh, PA, 1998.
- (27) Lee, J. E.; Choi, W.; Mhin, B. J. *Bull. Korean Chem. Soc.* **2003**, *24*, 792.
- (28) *CRC Handbook of Chemistry and Physics*, 77th ed.; Lide, D. R., Ed.; CRC Press: Boca Raton, FL, 1996; pp 7–71.
- (29) Scott, A. P.; Radom, L. *J. Phys. Chem.* **1996**, *100*, 16502.
- (30) Kim, K. S.; Mhin, B. J.; Choi, U.-S.; Lee, K. *J. Chem. Phys.* **1992**, *97*, 6649.
- (31) Pitzer, K. S.; Gwinn, W. D. *J. Chem. Phys.* **1942**, *10*, 428.
- (32) Choo, J.; Laane, J.; Majors, R.; Villarreal, J. R. *J. Am. Chem. Soc.* **1993**, *115*, 8396.
- (33) Chen, C.-C.; Lay, T. H.; Bozzelli, J. W. *J. Phys. Chem. A* **2003**, *107*, 6451.
- (34) Gastilovich, E. A.; Klimenko, V. G.; Korolkova, N. V.; Nurmukhametov, R. N. *Chem. Phys.* **2002**, *282*, 265.
- (35) *Calculated Molecular Properties of Polycyclic Aromatic Hydrocarbons*; Hites, R. A., Simonsick, W. J., Eds.; Elsevier: New York, 1987.